Plant Physiology and Biochemistry 207 (2024) 108403

Contents lists available at ScienceDirect

Plant Physiology and Biochemistry

journal homepage: www.elsevier.com/locate/plaphy

Growth, physiological parameters and DNA methylation in *Spirodela polyrhiza* (L.) Schleid exposed to PET micro-nanoplastic contaminated waters

Marco Dainelli [a], Maria Beatrice Castellani [b], Sara Pignattelli [b], Sara Falsini [a], Sandra Ristori [c], Alessio Papini [a], Ilaria Colzi [a,*], Andrea Coppi [a,1], Cristina Gonnelli [a,1]

[a] Department of Biology, Università degli Studi di Firenze, via Micheli 1, 50121, Florence, Italy
[b] Institute of Bioscience and Bioresources (IBBR), National Research Council (CNR), Via Madonna del Piano 10, 50019, Sesto Fiorentino, Italy
[c] Department of Chemistry, University of Florence, Via della Lastruccia 3, Sesto Fiorentino, 50019, Firenze, Italy

ARTICLE INFO

Handling Editor: Shivendra Sahi

Keywords:
Plastic pollution
Micro- and nanoplastics
DNA methylation
Oxidative stress
Duckweeds

ABSTRACT

The effects of polyethylene terephthalate micro-nanoplastics (PET-MNPs) were tested on the model freshwater species *Spirodela polyrhiza* (L.) Schleid., with focus on possible particle-induced epigenetic effects (i.e. alteration of DNA methylation status). MNPs (size ~ 200–300 nm) were produced as water dispersions from PET bottles through repeated cycles of homogenization and used to prepare N-medium at two environmentally relevant concentrations (~0.05 g L^{-1} and ~0.1 g L^{-1} of MNPs). After 10 days of exposure, a reduction in fresh and dry weight was observed in treated plants, even if the average specific growth rate for both frond number and area was not altered. Impaired growth was coupled with a MNP-induced decrease of chlorophyll fluorescence parameters (i.e. ΨET_o and Pi_{abs}, indicators of photochemical efficiency) and starch concentration, as well as with alterations in plant ionomic profile and oxidative status. The methylation-sensitive amplification polymorphism (MSAP) technique was used to assess possible changes in DNA methylation levels induced by plastic particles. The analysis showed unusual hypermethylation in 5′-CCGG sites that could be implicated in DNA protection from dangerous agents (i.e. reactive oxygen species) or in the formation of new epialleles. This work represents the first evidence of MNP-induced epigenetic modifications in the plant world.

1. Introduction

The last 70 years have seen the human society generating a global plastic crisis and prompting one of the most severe transboundary threats to the environment (Rivas et al., 2022). Based on available data (OECD, 2022), only 9 % of plastic waste is well taken over and recycled, while the rest is incinerated (19 %), landfilled (50 %) or ends up in natural ecosystems (22 %). In addition, the recent Covid-19 pandemic crisis has elicited the consumption of personal protective kits and other disposable items, furtherly bolstering plastics dispersion all over the globe (Kiran et al., 2022; Patrício Silva et al., 2021; Wang Q. et al., 2023). Nearly all of terrestrial, freshwater and marine ecosystems is contaminated by different types of plastic materials (i.e. polystyrene, polyethylene terephthalate, polyvinyl chloride etc.) that are degraded very slowly in nature, thus creating new emerging threats: microplastics (particles with a size <5 mm) and nanoplastics (size <0.1 μm) (Cui Q. et al., 2023; Wu et al., 2017; Yin et al., 2021). The ubiquitous presence of micro-nanoplastics (MNPs) and their potential availability to living organisms have attracted the attention of the scientific community, leading to many publications concerning their toxic or harmful effects (Anbumani and Kakkar, 2018).

Research has been mostly focused on animals in marine or tidal ecosystems (see e.g., Egbeocha et al., 2018; Miller et al., 2020 etc.) and only recently on terrestrial plants and animals (see e.g., Dey et al., 2023; Ilechukwu et al., 2022 etc.). More attention should be given to freshwater environments, which act as sinks for plastic particles by accumulating and transporting them from lands to seas and oceans (Besseling et al., 2017; van Weert et al., 2019). In this framework, aquatic vegetation has fundamental ecological functions, since it provides a habitat for different organisms and is implicated in vital processes, such as

* Corresponding author.
E-mail address: ilaria.colzi@unifi.it (I. Colzi).
[1] Co-last authors.

https://doi.org/10.1016/j.plaphy.2024.108403
Received 22 September 2023; Received in revised form 9 January 2024; Accepted 25 January 2024
Available online 27 January 2024

nutrient cycling, water cleaning, etc. (Bornette and Puijalon, 2009). In 2020 (a), (Kalčíková, 2020a) stated that these organisms are "a forgotten piece of nature" in the field of MNP research, paving the way for new efforts to bridge this knowledge gap. From that moment on, the impact of MNPs, alone or in combination with other contaminants, on various submerged macrophytes was considered, emphasizing their effects on growth and physiology (see e.g., Senavirathna et al., 2022; Wang L. et al., 2021; Yu et al., 2022; Zhou et al., 2022). Concurrently, information on free floating macrophytes is increasing (i.e., *Lemna* sp. and *Spirodela polyrhiza*), and these systems are often used in laboratory toxicity tests because of their small size, simple structure, asexual reproduction and short generation time (OECD, 2006). Polyethylene (PE) and polystyrene (PS) MNPs have been shown to adhere directly on the surfaces of the roots of *Lemna minor* and *Spirodela polyrhiza* without impairing growth, whereas their effective absorption has still to be confirmed (Dovidat et al., 2020; Mateos-Cárdenas et al., 2019). Similar results have been obtained by Kalčíková et al. (2020b) on *L. minor* exposed to PE-MNPs extracted from a proprietary body scrub. Wang Y. et al. (2023a) have reported that high doses (0.1 g L^{-1} and 1 g L^{-1}) of polyvinyl chloride (PVC)-MNPs can affect biometric and physiological traits of *S. polyrhiza* and these effects are coupled with relevant changes in primary and secondary metabolism. Interestingly, a long-term (12 weeks) exposure experiment of *L. minor* to cosmetic-derived PE-MNPs (0.1 g L^{-1}) has demonstrated that plastic particles alter the protein content and total antioxidant capacity of plants only during the first week of the test, thus highlighting a subsequent adaptation to the presence of pollutants (Rozman et al., 2022). Since plant adaptation to stressful conditions is mediated at the molecular level through differential gene expression that aims to reduce the adverse effects of stress and increase their tolerance (Raza et al., 2020), this last outcome raises exciting new questions about the biological processes implicated in the modulation of phenotypic plasticity to respond to such new generation of contaminants. Actually, the presence of MNPs has been reported to induce transcriptomic changes in vascular plants (see e.g., Martín et al., 2023; Teng et al., 2022; Wang J. et al., 2022; Wang Y. et al., 2022; Wang Y. et al., 2023b; Xiao et al., 2022) and hence an impact of plastic particles on the regulation of gene expression is expected. Various mechanisms may govern this process, including epigenetic regulation, a common trait among plants and other living organisms, which plays an important role in their adaptation to different environmental conditions (Thiebaut et al., 2019). Epigenetic modifications do not refer to changes in DNA sequence, but include DNA methylation, histone modifications and RNA interference (Thiebaut et al., 2019). Among these three factors, DNA methylation of cytosines at position 5 of the pyrimidine ring (5-Me-C) is widespread in the plant world, also helping to maintain genome stability (Vanyushin and Ashapkin, 2011; Zhang et al., 2018). DNA methylation is part of a complex interacting epigenetic network that controls gene activation or deactivation (Zhao et al., 2015). In this respect, accumulating evidence has demonstrated that DNA methylation can be altered at individual loci or across the entire genome under stress conditions (Zhang et al., 2018; Sun et al., 2021). To the best of our knowledge, MNP-induced alteration of DNA methylation patterns has been demonstrated only in animals (see e.g. Farag et al., 2023; Im et al., 2022) and the same holds true for other epigenetic mechanisms (López de las Hazas et al., 2022), highlighting the need to study how plant organisms cope with plastic particles through the modulation of DNA methylome.

Considering the above-reported importance of macrophytes in maintaining a good ecological balance in freshwater environments, *Spirodela polyrhiza* was used as a model plant to study MNP phytotoxicity. Moreover, any changes in the DNA methylation levels of this species would be of particular significance since its epigenome has an extremely low level of global DNA methylation (around 9 % of the genome) if compared to other species (e.g. *Arabidopsis thaliana* = 32 %) (Cao and Vu, 2020; Michael et al., 2017).

This work aims to evaluate the impacts of polyethylene terephthalate (PET)-MNPs at environmentally relevant concentrations (≈0.05 and 0.1 g L^{-1}, see e.g. Li C. et al., 2020) on the growth and physiology of *S. polyrhiza* with unprecedented attention to DNA methylation profiles. For this purpose, the methylation-sensitive amplification polymorphism (MSAP) technique was used, which is an approach based on specific isoschizomers differing for sensitivity with the methylation state of the cut site (i.e. 5′-CCGG sites) and allowing the comparison of large amounts of methylation-sensitive regions across the whole genome (Schrey et al., 2013). To the best of our knowledge, this is the first study that explores plastic-induced epigenetic changes in the plant world.

2. Materials and methods

2.1. Production and characterization of MNPs

Polyethylene terephthalate (PET) plastics were obtained by breaking down water bottles from an Italian producer using the protocol developed by Ekvall et al. (2019) with modifications. The bottle surface was previously washed with standard detergent for glassware to avoid contaminations (bacteria, proteins, nucleic acids, etc.), cut with scissors into pieces of 0.5 mm^2 each, and then flushed abundantly with deionized water. After drying and sterilizing by UV-C rays (250–280 nm; net irradiance 2280 W m^{-2}) for 1 h, 4 g of pieces were put in a beaker (Volume 1L) with 150 mL of distilled water. An immersion blender (Bosch ErgoMixx 600W -E-nr: MSM66020/1-, Robert Bosch GmbH) was used to break the plastic in water for 2 min at maximum speed. 50 mL of the solution were collected with a sterile syringe (Pentaferte Italia) and then filtered through a Miracloth filter (Calbiochem®) with pore size 22–23 μm. This cycle was repeated 20 times with 2 min pause after each cycle and 5 min after the 5th, 10th and 15th cycles, to avoid overheating. After collecting 1 L, each MNPs suspension was stored in a glass bottle at +4 °C. The amount of plastic in solution was calculated by subtracting the weight of debris collected at the end to the weight of the plastic at the beginning of the preparation. The size distribution of the particles was investigated by Dynamic Light Scattering (DLS) on a Malvern Zetasizer Nano ZS (ZEN 1600 model, Malvern Instruments Southborough, MA), equipped with He–Ne 633, 4 mW laser with backscattering detection. Detector attenuation was set at 10 to allow quantitative comparison among different samples. DLS measurements were performed over 11 runs and in duplicate and showed that the mean size of the MNPs was in the range 180–250 nm. Fig. S1 and Table S1 reports the results obtained for two independent specimens from the same preparation. The polydispersity index (PDI) was between 0.4 and 0.5. This revealed a broad size distribution, which was however monomodal and allowed an estimate of the item number as 1.5 x 10^7 particles/mL. Such value was obtained by approximating the particle shape to spheres and can be considered adequate for this kind of experiments (Song et al., 2020). Zeta Potential (ζ) measurements were performed on a Zetasizer (Zetasizer Pro, Malvern Panalytical Co. Ltd., Malvern, UK) in DTS1070 cells, at 25 °C. The ζ values were measured in a mixed mode, using phase analysis light scattering (M3-PALS). Each measurement was repeated two times, and values are reported as the mean with their - standard deviation over 15 runs. The surface of the MNPs obtained was negatively charged. In particular, the average ZP values were around −10 mV (Table S1). This indicated moderate, but not negligible, absorbing capability toward different chemical species, as it is widely reported in the literature for particles with similar surface charge (My Tran et al., 2021; Sitko et al., 2013). Moreover, the measured surface charge of the submicron plastic particles, though not very high in absolute value, ensured the stability of water dispersions by electrostatic repulsion.

2.2. Plant growth and experimental conditions

The effects of the above-described PET-MNP solution were tested on the freshwater floating plant species *Spirodela polyrhiza* (L.) Schleid.

following the OECD guidelines for the testing of chemicals (Test n°221, 2006) with slight modifications. *S. polyrhiza* strain 9509, gently provided by the University of Jena (Germany), was acclimated for two weeks before testing in a climate chamber with the following controlled conditions: 24/16 °C day/night, light intensity 300 μmol m^{-2} s^{-1}, 16-h (day) photoperiod and relative humidity 60–65 %. The vessels used for axenic cultivation were 100 mL Erlenmeyer flasks with cotton wool stoppers containing 50 mL of the N-medium growing solution (Appenroth et al., 1996). After acclimation, one flask was used as inoculum culture (hereafter T0) and one colony (2–4 fronds) was randomly transferred from it to each test vessel. The latter were the same kind of Erlenmeyer flasks with cotton wool stoppers mentioned before. Three different treatment conditions were applied: *i)* control (C), 50 mL N-medium prepared in distilled water; *ii)* 50 mL N-medium prepared in PET-MNP solution diluted 1:2 (v/v) with distilled water (PET ½, MNP concentration ≈ 0.05 g L^{-1}); *iii)* 50 mL N-medium prepared in pure PET-MNP solution (PET, approximative MNP concentration ≈ 0.1 g L^{-1}). The number of replicates per treatment group was 16, for a total of 48 test vessels. The particle concentrations used in this experiment were comparable to those reported for contaminated freshwaters (see e.g. Gupta et al., 2022; Li C. et al., 2020). No contamination was observed during the exposure test that lasted 10 days from inoculation in static conditions. As for growth parameters, total frond area (expressed in cm^2) and total frond number of *S. polyrhiza* were monitored at the beginning and at the end of the test. A digital camera (Canon PowerShot SX100 IS), placed at a distance of 5 cm from the top of the flasks, was used to take pictures of the colonies. The images were then analysed with Fiji software of ImageJ (Schindelin et al., 2012) and the average specific growth rate (μ) for both growth parameters was calculated according to OECD (2006) with the following formula: $\mu_{i\text{-}j} = (\ln (N_j) - \ln (N_i))/t$, where t is the time period from time i (day 0 from inoculation) to time j (day 10 from inoculation) and N_i/N_j are the measurable variables in the test or control vessel at time i and time j. At the end of the treatments, plants were carefully washed three times with MilliQ water and blotted dry on filter paper. Fresh and dry weights of all plants from a subset of test flasks (8 per treatment group) were also determined, while the rest of the material was used for the analysis described in sections 2.3, 2.5 and 2.6.

2.3. Chlorophyll fluorescence analysis

Chlorophyll *a* fluorescence was measured on one colony per flask at day 10 after inoculation using a portable fluorimeter (HandyPEA, Hansatech Instruments Ltd, Norfolk, UK). HandyPEA leafclips were used to dark-adapt *S. polyrhiza* for 15 min, taking care that the plants did not dry out by placing them on absorbent paper wetted with distilled water. A 1-s long saturating light pulse (3500 μmol m^{-2} s^{-1}, 650 nm) was then applied by the sensor of the fluorimeter and the fluorescence emission recorded, thus obtaining OJIP transients to be analysed. These transients were analysed according to Stirbet and Govindjee (2011) after double normalization between F_0 (step O, minimum fluorescence value at 20 μs) and F_M (plateau P, maximum fluorescence value at plateau). Double normalized transients were used to calculate basic selected parameters (listed and described in Table S2) with the Biolyzer software (Fluoromatic Software, Geneva, Switzerland) and to coherently compare the different treatment groups.

2.4. Starch concentration determination

Starch concentration was determined with the colorimetric method proposed by Appenroth et al. (2010). Briefly, 200 mg of fresh plant material was manually crushed and homogenised in 4 mL 18 % (w/v) HCl with the aid of glass mortar and pestle. The mixture was then shaken for 1 h at 4 °C and immediately centrifuged at 12.000 rpm for 20 min. The supernatant was mixed with Lugol's solution (KI 0.5 % w/v and I_2 0.25 % w/v in distilled water) in 1:1 ratio and the absorbance was measured at 605 nm and 530 nm with a UV/Vis spectrophotometer (Lambda 35, PerkinElmer). The amount of starch per fresh weight (S%, w/w) was calculated with the formulae reported and described by Appenroth et al. (2010) and Rana et al. (2021). Starch concentration was determined on 6 replicates per treatment group at the end of the test and on 3 replicates from the inoculum culture.

2.5. Ionome analysis

The elemental profile of *S. polyrhiza* plants was determined according to already standardized methodologies (i.e. Bettarini et al., 2019). Oven-dried plant material (50 °C for 48 h) was acid-digested using 10 mL of 69 % HNO_3 in a microwave digestion system (Mars 6, CEM) with maximum temperature of 200 °C for 20 min. Element concentrations (K, Ca, Mg, Fe, Zn, Mn, Na, Cu and Ni) were measured by atomic absorption spectroscopy (PinAAcle 500, PerkinElmer) verifying the reliability (<10 % RSD) and accuracy (<5 % RSD) of the method with certified reference materials (grade BCR, Fluka Analytical, Sigma-Aldrich). Macro- and micronutrient concentrations were then expressed on a dry weight basis as mg g^{-1} and μg g^{-1} respectively.

2.6. Hydrogen peroxide, malondialdheyde and antioxidants quantification

Plant material was sampled (5 replicates of about 200 mg per treatment group) and extracted in trichloroacetic acid (TCA) after powderization in liquid nitrogen. The extracts were then used to determine hydrogen peroxide (H_2O_2), malondialdheyde (MDA) and antioxidants (glutathione and ascorbic acid). The method proposed by Alexieva et al. (2001) was used for H_2O_2 determination and consisted in a reaction with 1 M potassium iodide (KI) in the presence of 10 mM potassium phosphate buffer (pH 7.8). The reaction mixture was incubated for 1 h in the dark and then the absorbance at 390 nm was recorded. H_2O_2 concentration was calculated using a calibration curve prepared with known H_2O_2 concentrations and the results were expressed as μg g^{-1} fresh weight. Thiobarbituric acid (TBA) method (Heath and Packer, 1968) was employed to determine MDA concentration: an aliquot of TCA extracts was mixed with the same amount of 0.5 % TBA in 20 % TCA and immediately heated at 95 °C for 30 min. The reaction was then stopped by rapidly cooling down the mixture at −20 °C for 5 min. The absorbance of the supernatant obtained after centrifugation at 10.000×*g* for 10 min was measured at 532, 600 and 450 nm in order to calculate MDA concentration with the following formula: C (μmol L^{-1}) = 6.45 ($A_{532} - A_{600}$) - 0.56 A_{450}. The results were expressed in μmol g^{-1}. As for glutathione (GSH), the absorbance of the extracts was read at 412 nm after reaction with 0.01 M Ellman's reagent (5,5′-dithiobis-(2-nitrobenzoic acid) or DTNB) in the presence of Tris-EDTA buffer (pH 8.2), following the method by Sedlak and Lindsay (1968) with slight modifications. A standard curve was prepared with known GSH concentrations and the results were expressed as μg g^{-1} fresh weight. Ascorbic acid (AsA) concentration was measured with an assay that is based on the reduction of Fe^{3+} to Fe^{2+} in acidic solution (Law et al., 1983); the reduced form reacts with bipirydyl giving a specific colour with a maximum absorbance at 525 nm. AsA concentrations (μg g^{-1} fresh weight) were determined by comparison with a standard curve, as was done for H_2O_2 and GSH. All measurements were performed with a UV/Vis spectrophotometer (Lambda 35, PerkinElmer).

2.7. DNA extraction and Methylation Sensitive Amplified Polymorphism (MSAP) analysis

A total of 32 samples (about 200 mg fresh weight per sample) was collected for genomic DNA extraction and includes: *i)* 8 samples from the T0 inoculum culture, collected at the beginning of the exposure test (0 days from inoculation); *ii)* 8 samples for each treatment group (C, PET ½ and PET), collected at the end of the exposure test from different flasks

(10 days from inoculation).

Genomic DNA was extracted, within one week from collection time, from plant tissues, dried in silica gel at room temperature, with Quick-DNA™ ZR Plant/Seed Miniprep Kit (Zymo Research, California, USA) following the manufacturer's protocol. Quality and quantity control of extracted DNA were estimated by using Bio-Photometer (Eppendorf, Germany).

MSAP protocol is similar to that of traditional Amplified Fragment Length Polymorphism (AFLP) technique (Vos et al., 1995), but requires the use of two methylation-sensitive isoschizomeric enzymes, MspI and HpaII. They both recognize 5′-CCGG sequences, but differ in their sensitivity to the methylation state of the internal and external cytosine residues (Chwialkowska et al., 2017; Schrey et al., 2013; Thiebaut et al., 2019). Standard MSAP protocol is usually performed combining these two enzymes with the classical rare cutter EcoRI in two separate amplifications, in which appropriate adaptors and primers are used according to each restriction enzyme. In this way it's possible to compare the resulting fragment profiles and detect the methylation state of different 5′-CCGG sites (loci) (Schrey et al., 2013; Schultz et al., 2013). However, since EcoRI enzyme is partially sensitive to methylation and may show reduced cleavage in some cases, we decided to use MseI, whose cleavage site does not contain any cytosine residue, as suggested by Medrano et al. (2014).

Therefore, in the first reaction, genomic DNA (200 ng) of each sample was digested with 20 units of MseI (NEB, United States) and 25 units of MspI (NEB) for 2 h at 37 °C in a total volume of 25 μL, using the manufacturer's buffer. In the second digestion reaction, HpaII was used instead of MspI. All digested fragments were then ligated with 50 pmol double-strand oligonucleotide adapters (MseI and HpaII/MspI) for 2 h at 20 °C. Amplification was performed by using 5 μL of 1:2 diluted ligation mixture in a final volume of 25 μL containing 2.5 μl of 10x reaction buffer (Dynazyme II; Finnzyme, Espoo, Finland), 1.5 mM $MgCl_2$, 200 μM of deoxynucleoside triphosphates, 1U of Taq DNA polymerase (Dynazyme II; Finnzyme) and 10 pmol of each of primer. As a first step, four primer-pair combinations (Table S3) were tested on four samples (one from each treatment group) to assess the combination that produced the most readable and informative profiles. Through this, two combinations of primers, hex_HM-TTC/MseI-ATG and fam_HM-TAA/MseI-ATG, were selected for the final analysis since they produced highly repeatable MSAP profiles (error rates 0.9–1 %) from 21 samples (ca. 65 % of the entire data set). PCR reactions were performed with the following profile: 94 °C for 1 min, followed by 12 cycles of 94 °C for 30 s, 65 °C for 30 s, and 72 °C for 1 min, followed by further 23 cycles of 94 °C for 30 s, 56 °C for 30 s, 72 °C for 1 min, and final extension at 72 °C for 2 min. No preselective PCR reaction was performed before amplification with selective primers, following MSAP protocols by Alonso et al. (2016) and Medrano et al. (2014). This choice was supported by the high repeatability of MSAP profiles and the good number of obtained fragments with the above-mentioned combinations of primers. The amplification products were separated by capillary electrophoresis using the ABI310 Genetic Analyzer (Applied Biosystem, FosterCity, CA, USA).

2.8. MSAP data analysis

MSAP profiles generated by capillary electrophoresis (please see Supplementary Material_1, Fig. S2) were analysed using GeneMarker v1.5 (SoftGenetics LLC, State College, PA, United States). A cut-off value (5 % of the maximum profile in the chromatograms) for band attribution was fixed after analysis of replicate samples, considering only bands present in all replicates. Densitometric profile of each chromatogram was then inspected to check and correct the detected bands. The MSAP raw data (Supplementary Material_2) were scored following the protocol proposed by Schulz et al. (2013). Four different conditions could be identified for each fragment: *i)* unmethylated state (U, i.e. fragment is present in both HpaII-MseI and MspI-MseI products); *ii)* hemimethylated external cytosine (^{HMe}CCG, i.e. fragment is present only in HpaII-MseI products) *iii)* full- or hemimethylated internal cytosine (^{Me}CG and ^{HMe}CG, i.e. fragment is present only in MspI-MseI products) and *iv)* uninformative state (i.e. absence of fragment in both HpaII-MseI and MspI-MseI products) (Alonso et al., 2016; Schulz et al., 2013). This last condition could be caused by either hypermethylation or mutation of the restriction site and, being uninformative, was not considered in the comparisons of MSAP profiles (Alonso et al., 2016; Schulz et al., 2013).

The transformation and scoring of data were performed using the model "Mixed Scoring 2" and the MSAP raw data table (Supplementary Material_2) as input, following Schulz et al. (2013). Using the R script MSAP_calc, each locus of the raw data table was split into one to three subloci (i.e. markers) according to the different states in which it appears through the samples, allowing a separate analysis for each of the above-mentioned conditions. The generated epigenetic data matrices (one for each of the conditions) are included in Supplementary Material_3. The epigenetic diversity metrics (Table 2) were obtained using the R script MSAP_calc as well, while the number and the relative percentage (number of markers per sample/total number of markers; %) of loci in different conditions (U-loci, ^{HMe}CCG-loci, ^{Me}CG- and ^{HMe}CG-loci) for each sample was calculated manually from the output data matrices in Supplementary Material_3.

2.9. Statistics

Concerning growth parameters (i.e. average specific growth rates, fresh and dry weight) and physiological parameters (i.e. chlorophyll fluorescence, starch and element concentration, H202, MDA, GSH and AsA concentration), the One-way ANOVA was used to check the significance of differences ($P < 0.05$) among means of treatment groups, using GraphPad Prism 7 (GraphPad Software, San Diego, CA). Data normality was checked with the Shapiro-Wilk test, whereas the Bartlett's test was used for checking homogeneity of variances.

Differences among treatment groups in terms of epigenetic diversity metrics were evaluated with the same statistical test. In addition, patterns of epiloci differentiation were tested by the Analysis of Molecular Variance (AMOVA), using Arlequin software (Excoffier and Lischer, 2010).

3. Results

3.1. Effects of MNPs on plant growth and photosynthesis

The presence of PET-MNPs in the growing medium did not impair the growth of *S. polyrhiza* in terms of variation in average specific growth rate of both frond number and area (Fig. 1a and b). Despite this, plants treated with both MNP concentrations showed significantly reduced values of fresh and dry weight (Fig. 2a and b, $F = 7.325$, $P = 0.0041$ and $F = 7.418$, $P = 0.0039$ for fresh and dry weight, respectively). Chlorophyll fluorescence analysis demonstrated that most of the considered OJIP-test parameters (Table 1, F_0, ΦP_o, ΨRE_o, Sm and ABS/RC) did not significantly change upon plant growth in MNP solutions, with the only exception of ΨET_o (i.e. the probability of which a PSII-trapped electron is transferred beyond reduced QA, or estimate of the oxidized-plastoquinone size; Bussotti et al., 2012; Colpo et al., 2023; Strasser et al., 2000; Table S1) and Pi_{abs} (i.e. the potential ability for energy conservation, from absorbed photons in PSII to the reduction of electron acceptors; Bussotti et al., 2012; Colpo et al., 2023; Strasser et al., 2000; Table S1) values that were significantly reduced in samples treated with the highest PET concentration (Table 1, $F = 7.004$, $P = 0.0047$ and $F = 4.735$, $P = 0.0207$ for ΨETo and Pi_{abs} respectively).

3.2. Effects of MNPs on starch and element concentration

Starch concentration (% dry weight) was significantly reduced in MNP-treated plants ($C = 4.69 \pm 0.19$, PET ½ $= 3.79 \pm 0.38$, PET $= 3.06 \pm 0.71$; $F = 18.53$, $P < 0.0001$), by about a fifth in PET ½ plants and a

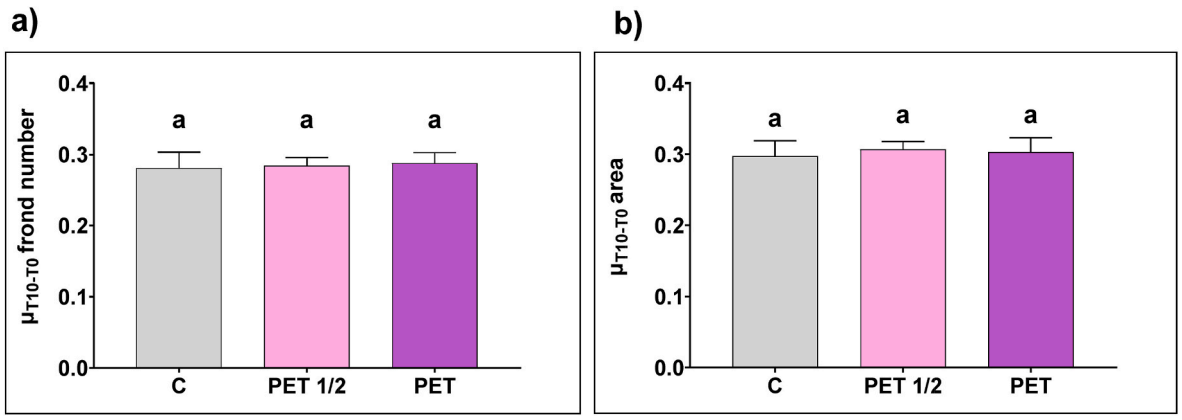

Fig. 1. Average specific growth rate (μ_{T10-T0}) of *a)* frond number and *b)* area of *S. polyrhiza* plants grown in absence (C) or in presence of MNPs at different concentrations (PET ½ and PET). Values are mean of 16 replicates ± standard deviation. Lower case letters indicate significant differences among the samples (at least $p < 0.05$).

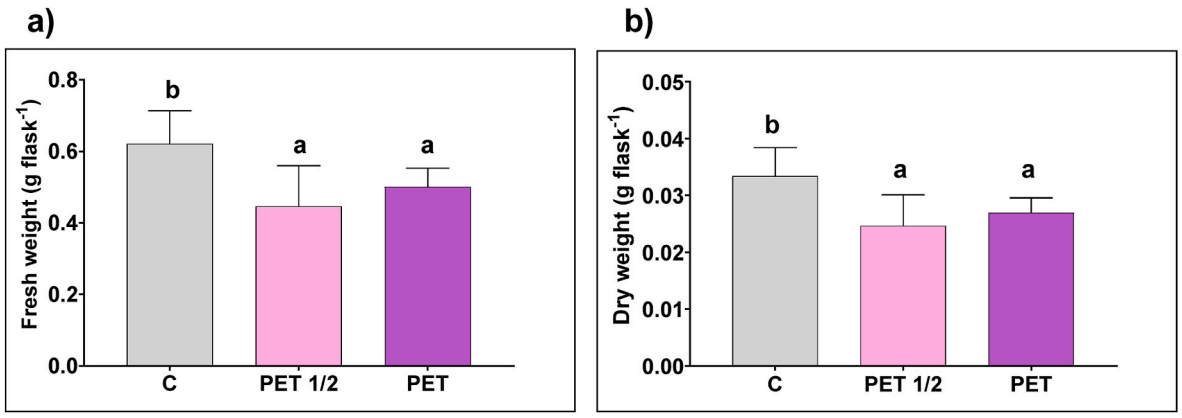

Fig. 2. *a)* Fresh and *b)* dry weight of *S. polyrhiza* plants grown in absence (C) or in presence of MNPs at different concentrations (PET ½ and PET) for ten days. Values are mean of 8 replicates ± standard deviation. Lower case letters indicate significant differences among the samples (at least $p < 0.05$).

Table 1
Values of OJIP-test parameters of *S. polyrhiza* plants grown in absence (C) or in presence of MNPs at different concentrations (PET ½ and PET) for ten days. Values are mean of 8 replicates ± standard deviation. Letters indicate the significant differences among the treatments (at least $p < 0.05$).

OJIP-test parameter	Treatments								
	C			PET 1/2			PET		
F_0	573.571	±	42.442 a	583.000	±	31.541 a	577.250	±	32.473 a
ΦP_o	0.752	±	0.018 **a**	0.752	±	0.012 **a**	0.745	±	0.013 **a**
ΨET_o	0.517	±	0.017 **b**	0.509	±	0.017 **b**	0.486	±	0.016 **a**
ΨREo	0.256	±	0.024 **a**	0.268	±	0.021 **a**	0.252	±	0.014 **a**
Sm	30.179	±	3.206 **a**	31.189	±	2.511 **a**	29.259	±	2.113 **a**
ABS/RC	4.331	±	0.280 **a**	4.078	±	0.318 **a**	4.124	±	0.284 **a**
Pi_{abs}	8.343	±	1.206 **b**	7.780	±	0.816 **ab**	6.779	±	0.980 **a**

third in PET plants in respect to control samples.

Concerning macro-elements, K and Ca concentration was not significantly changed after the exposure to PET-MNPs (Tables S4 and F = 1.527, P = 0.2402 and F = 0.6613, P = 0.5266 for K and Ca respectively). Magnesium (Mg) was the only macronutrient that showed an increase in concentration in MNP-exposed plants with respect to control plants, significantly for PET ½ plants with respect to control plants (Tables S4 and F = 9.803, P = 0.0010). Regarding micro-elements, Mn and Na concentration was significantly higher in MNP-treated plants as compared with control plants (Tables S4 and F = 6.553, P = 0.0061 and F = 18.76, P < 0.0001 for Mn and Na respectively), whereas Zn concentration did not change among treatments. No significant differences between control and MNP-treated plants were reported also for Fe, Cu and Ni concentrations.

Fig. 3 represents the amplitude heatmap of the MNP-treatment-induced increase/decrease in element concentration. Overall, the ionome of PET ½ plants was more altered than that of PET plants, with a notable increase in Mg, Mn and Na levels. In general, the differences were more marked for micro-elements with respect to macro-elements.

3.3. Effects of MNPs on plant oxidative status

Plants grown with PET-MNPs in the culture medium at the highest concentration showed a significantly higher amount of H_2O_2 and GSH (Fig. 4a and b, F = 9.320, P = 0.0023 and F = 31.01, P < 0.0001 for H_2O_2 and GSH respectively). Conversely, MDA concentration was

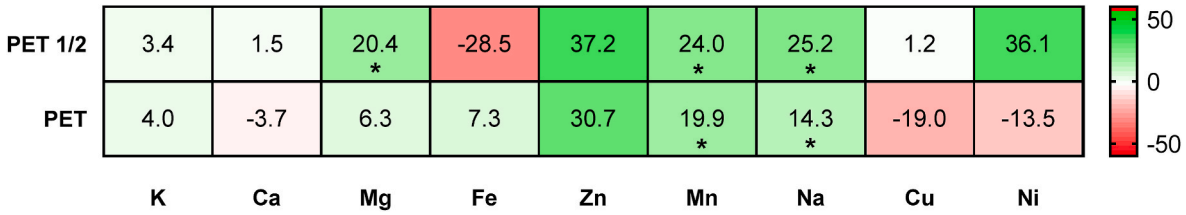

Fig. 3. Heatmap showing ionome variation of *S. polyrhiza* plants grown in presence of MNPs at different concentrations (PET ½ and PET) for ten days. Colour scale indicates decreased (red), unchanged (white) or increased (green) element concentration in respect to the control. The percentage of variation is reported, together with asterisks indicating the significant difference between the element concentrations in treated and control plants (at least $p < 0.05$).

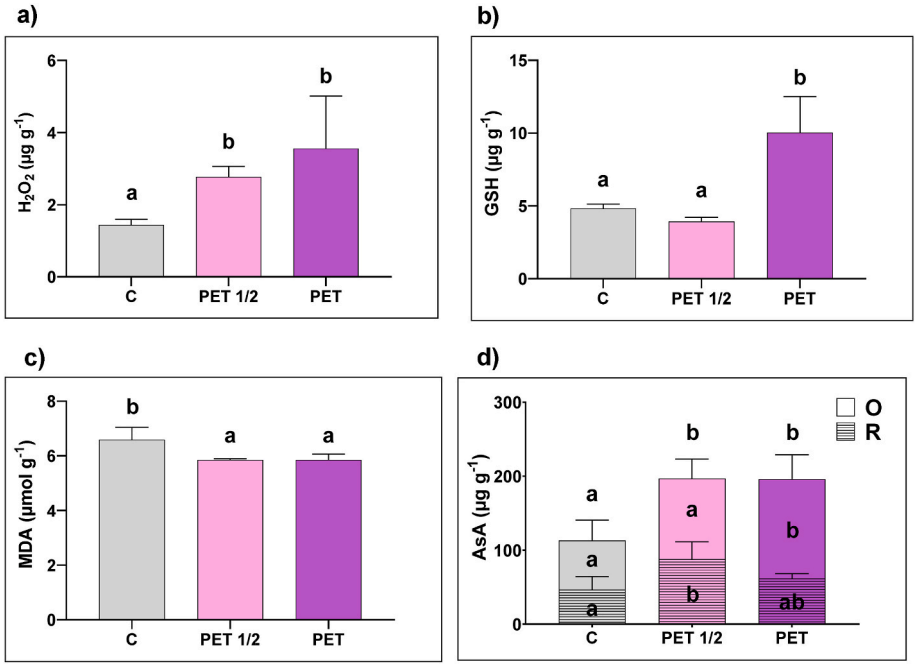

Fig. 4. Concentration of *a)* H_2O_2 (µg g^{-1}), *b)* GSH (µg g^{-1}), *c)* MDA (µmol, g^{-1}) and *d)* AsA (µg g^{-1}), total, oxidized (O) and reduced (R), in *S. polyrhiza* plants grown in absence (C) or in presence of MNPs at different concentrations (PET ½ and PET) for ten days. Values are mean of 6 replicates ± standard deviation. Lower case letters indicate significant differences among the samples (at least $p < 0.05$).

significantly lower in PET ½ and PET plants with respect to control plants (Fig. 4c–F = 12.57 and P = 0.0006). Concerning AsA, treated plants showed a higher total concentration (reduced plus oxidized form; Fig. 4d–F = 8.097 and P = 0.0041) in respect to control samples. Considering only the reduced form, its concentration was significantly higher in PET ½ plants (Fig. 4d–F = 8.511 and P = 0.0034), while the amount of the oxidized form was significantly higher in PET plants (Fig. 4d–F = 7.288 and P = 0.0061), always as compared to control samples.

3.4. MSAP results

Table 2 shows all the parameters describing the epigenetic markers found in the treatment groups for each of the conditions, all together or individually (Section 2.8). Using the R script MSAP_calc, the 196 loci of the MSAP raw data table (Supplementary Material_2) were transformed and scored into 497 subloci, representing the total informative markers for the three different conditions (U; ^{HMe}CCG; ^{Me}CG and ^{HMe}CG) considered together (Supplementary Material_3). Generally, PET ½ treated plants showed the highest percentage of polymorphic loci (63.8), followed in order by PET (59.4), C (55.7) and T0 (51.7). A total of 177 unmethylated loci (U-loci) were identified among the treatment groups. Significantly higher values (F = 14.63 and P < 0.0001) were detected for T0 (mean number of U-loci = 107; 60.5 %) and C (mean number of U-loci = 103; 58.0 %) with respect to PET ½ (mean number of U-loci = 84; 47.2 %) and PET (mean number of loci = 74; 42 %), Fig. 5a. The total number of loci with hemi-methylation of external cytosine (^{HMe}CCG-loci) were 172. The highest mean number was in PET 1/2 (mean number of ^{HMe}CCG-loci = 39; 22.7 %). This mean value was significantly higher (F = 5.038 and P = 0.0065) than that of T0 (mean number of ^{HMe}CCG-loci = 16; 12.3 %) and C (mean number of ^{HMe}CCG-loci = 21; 9.6 %), Fig. 5b. The total number of loci with full- or hemi-methylation of internal cytosine (^{Me}CG- and ^{HMe}CG-loci) was 148. The highest mean number was in T0 (mean number of ^{Me}CG- and ^{HMe}CG-loci = 19; 12.7 %), whereas the lowest number on average was in PET (mean number of ^{Me}CG- and ^{HMe}CG-loci = 11; 7.4 %); T0 mean value was significantly higher (F = 5.680 and P = 0.0040) than that of PET ½ and PET (Fig. 5c).

AMOVA showed that the most considerable portion of epigenetic differentiation was described within treatment groups (67.1 %; Table S5a). Nevertheless, a significant fraction of differentiation was described also by the differences among treatment groups (32.9 %). Dividing the treatment groups into two sub-groups (T0 and C versus PET ½ and PET), AMOVA showed that the most considerable amount of epigenetic variation among groups (31.1 %, Table S5b) can be attributed to the presence of PET-MNPs in the growth medium.

Table 2
Epigenetic metrics obtained with the R script MSAP_calc for all, ^{HMe}CCG (h), ^{HMe}CG & ^{Me}CG (m) and unmethylated loci (u). N_samples = number of samples per treatment group; N_markers_total = total number of markers in data set; N_markers_pop = number of markers present (with at least one "1"-score) per treatment group; N_markers_poly = number of polymorphic markers per treatment group; Pc_markers_poly = percentage polymorphic markers per treatment group; Mean_N_1scores = mean number of marker presence ("1"-scores) per treatment group; N_private_markers = number of private markers per treatment group, i.e. markers that only occur in this treatment group.

Treatment group	N_samples	N_markers_total	N_markers_pop	N_markers_poly	Pc_markers_poly	Mean_N_1scores	N_private_markers	h_N_markers_total	h_N_markers_pop	h_N_markers_poly	h_Pc_markers_poly	h_Mean_N_1scores	h_N_private_markers	m_N_markers_total	m_N_markers_pop	m_N_markers_poly	m_Pc_markers_poly	m_Mean_N_1scores	m_N_private_markers	u_N_markers_total	u_N_markers_pop	u_N_markers_poly	u_Pc_markers_poly	u_Mean_N_1scores	u_N_private_markers
T0	8	497	310	257	51,7	2,35	21	172	88	88	51,2	0,98	7	148	70	70	47,3	0,96	10	177	152	99	55,9	4,84	4
C	8	497	315	277	55,7	2,13	29	172	74	74	43	0,77	3	148	91	91	61,5	0,93	24	177	150	112	63,3	4,47	2
PET ½	8	497	341	317	63,8	2,17	37	172	122	122	70,9	1,81	9	148	69	69	46,6	0,65	21	177	150	126	71,2	3,78	7
PET	8	497	314	295	59,4	1,89	26	172	122	122	70,9	1,49	15	148	54	54	36,5	0,59	8	177	138	119	67,2	3,36	3

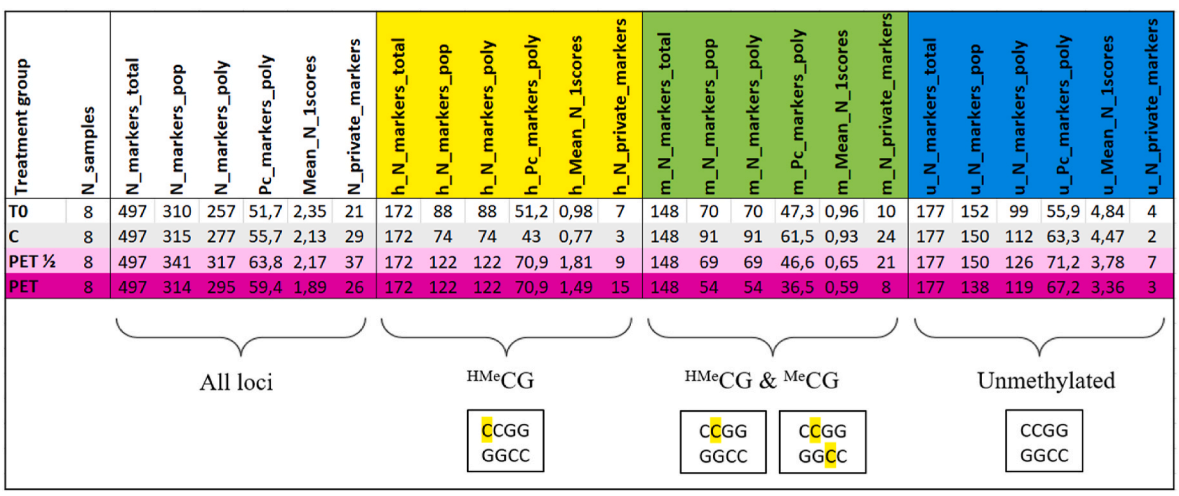

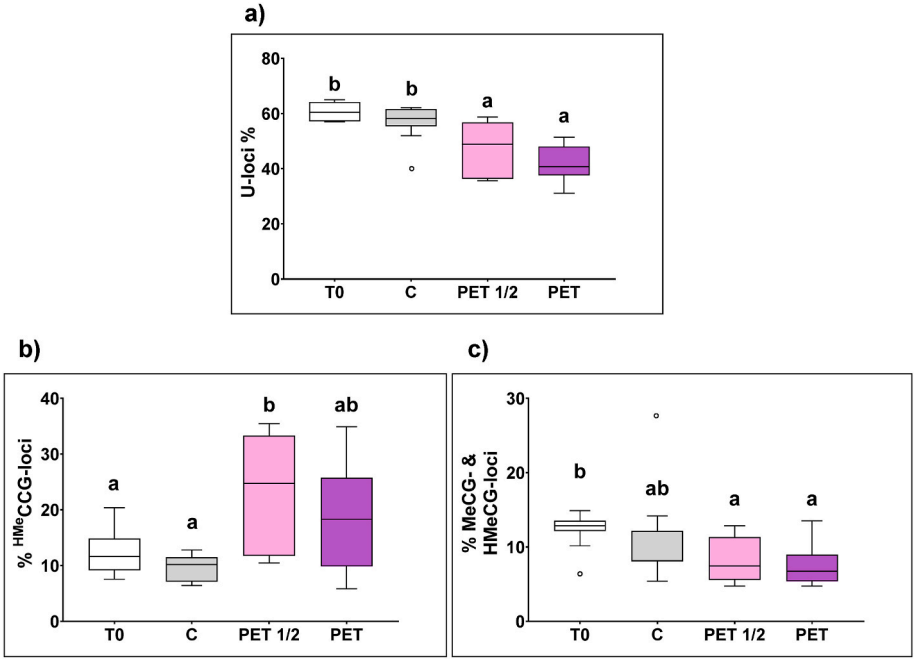

Fig. 5. Ratio (number of markers per sample/total number of markers; %) of *a)* unmethylated loci (U-loci), *b)* loci with hemi-methylation of external cytosine (^{HMe}CCG-loci) and *c)* loci with full- or hemi-methylation of internal cytosine (^{Me}CG- and ^{HMe}CG-loci) in the DNA of *S. polyrhiza* plants from the inoculum culture (T0) and after ten days of growth in absence (C) or in presence of MNPs at different concentrations (PET ½ and PET). Values are mean of 8 replicates ± standard deviation. Lower case letters indicate significant differences among the samples (at least $p < 0.05$).

4. Discussion

4.1. MNP exposure impacts on plant growth and physiological parameters

The average specific growth rate, for both frond number and frond area, was not impaired by the presence of environmentally realistic concentrations of PET particles. The lack of MNP effect on such biometric parameters was in accordance with other works in which *S. polyrhiza* was exposed to PS-MNPs of 50 and 500 nm (10^2 - 10^6 particles mL^{-1}, Dovidat et al., 2020) and PE-MNPs of 40–48 μm (0.4 g L^{-1}, Iannilli et al., 2023), and in contrast with exposure to PVC-MNPs of about 4 μm (0.01–1 g L^{-1}, Wang Y. et al., 2023a), probably due to the higher harmfulness of this last polymer to plants (Colzi et al., 2022; Dainelli et al., 2023; Falsini et al., 2022). Despite this apparent negligible toxicity of the plastic particles on plant development, PET-MNPs induced a significant decrease in both fresh and dry weight (mean % reduction = 24 % and 23 %, respectively) irrespective of the particle concentration. This result indicated that the effects of the tested pollutant can be variable depending on the considered growth parameter, and therefore that multiple biometric traits must be taken into

account when evaluating MNP toxicity on plants, as already demonstrated by Dainelli et al. (2023). In any case, the MNP-imposed decrease in *S. polyrhiza* weight might be partially explained by an impairment of the photosynthetic process in presence of plastic particles in the culture medium. If considering OJIP-test parameters like F0, FM, ΦP_o and others, no significant variations were observed among the treatment groups, coherently with a recent study by Cui R. et al. (2023) in which another duckweed species (i.e. *L. minor*) was exposed for different times to PET-MNPs of various sizes. However, the mean values of ΨETo and Pi_{abs} (see Table S2 for definitions) appeared reduced in treated plants, suggesting a decline in the functionality of the photosynthetic electron chain with an unavoidable expected decrease in organic matter accumulation (Bussotti et al., 2012; Colpo et al., 2023; Strasser et al., 2000). Accordingly, the concentration-dependent reduction of starch concentration reported in plants grown in presence of PET-MNPs confirmed a lower availability of photosynthates, thus limiting their polymerization in insoluble grains. This decline in starch levels could result dangerous to the reproductive potential of *S. polyrhiza* over long periods. In fact, this species survives to the unfavourable seasons by forming vegetative propagules, called turions, that accumulate a great quantity of starch granules (Xu et al., 2018). These dormant structures germinate in spring and the degradation of starch supports the rapid spread of the new fronds on the water surface (Appenroth et al., 2011). The MNP-induced decrease in starch concentration, already reportable in a short time exposure experiment like ours (i.e. 10 days), could suggest that longer exposures, encompassing the entire annual life cycle as it happens in nature, may result in a more profound alteration in starch storage, even in turions. Thereby, their germination rate and their capability to support the growth of novel vegetative tissues could be affected, thus amplifying the threat that plastic particles pose to such macrophytes and to the whole ecosystem.

Concerning element concentrations in MNP-treated samples, a few available studies report variable ionome alterations in plants exposed to plastic particles, in both pot and hydroponic systems, due to still unclear mechanisms (see for example Colzi et al., 2022; Dainelli et al., 2023; Fu et al., 2022; Tang et al., 2022). Regarding free floating macrophytes, information is not yet available; nonetheless, our result suggested that in such plants the effects of MNP pollution on the ionomic profile could be limited, at least in the short time. Actually, the only significant changes imposed by the presence of PET-MNPs was an increase in the accumulation of Mn, Na and, only for the lowest treatment concentration, Mg. *Spirodela polyrhiza* has a particular nutritional strategy in which the abaxial surface of the fronds performs nutrient and water uptake, while roots are mainly involved in floating and anchoring (An et al., 2019). Since most plastic particles have been shown to adhere to *S. polyrhiza* roots and not to the fronds (Dovidat et al., 2020; Wang Y. et al., 2023a), their impact on nutrient accumulation can be expected to be restricted. Moreover, PET particles are not supposed to massively float on the water surface due to their high density (>1.2 g cm^{-3}) (Monteiro and Pinto da Costa, 2022), thus probably not fully interfering with the abaxial surface of the fronds. In confirmation of this, the measured concentration of all the elements in all the treatment groups was comparable to those reported by Oláh et al. (2023) in different duckweed species under controlled conditions. Besides, the MNP-driven increase in the plant concentration of Na, Mg and Mn could be attributed to the co-occurrence of multiple factors, from the capacity of plastics to adsorb metals on their surface, acting thus as vectors (Squadrone et al., 2021; Zhang et al., 2021), to their imposed changes in the activity of ion transporters (Lian et al., 2022). Regarding the impact of a high tissue concentration of Mg and Mn, even if *S. polyrhiza* has been shown to be able to tolerate and accumulate high amounts of such elements (Liu et al., 2017; Schreinemakers, 1984), their probable further increase at longer exposure times could become limiting for plant growth. The same applies for a high tissue Na concentration, in accordance with Tang et al. (2022) who showed a similar increment in seedlings of *Oryza sativa* L. treated with PE-MNPs in hydroponics, and suggested an accumulation of this element to be of potential danger for the maintaining of the Na/K cellular equilibrium. In any case, the PET-imposed simultaneous excess of Na, Mg and Mn, cumulated to the still not significant variations in the other tested elements, could have thus concurred to determine the limitation in *S. polyrhiza* growth.

Regarding oxidative stress markers, MNP treatment induced an increase in H_2O_2 concentration, as already reported for other polymers and other free floating macrophytes with an extensive assessment of the ability of plastic particles to trigger reactive oxygen species (ROS) production, even though with still uncertain mechanisms (see e.g. Arikan et al., 2022; Gomes et al., 2023; Xiao et al., 2022). Contrarily to the just mentioned studies, in *S. polyrhiza* the increase in H_2O_2 was not coupled to an increase in MDA concentration, but to a significant decrease. The lack of oxidative stress damage could indicate that the presence of MNP-induced ROS, like H_2O_2, was triggering an excessive antioxidative response that resulted in a lower degree of lipid peroxidation in treated plants, at least for the plastic particle concentrations and exposure times used for this experiment. The increase in the concentration of reduced glutathione and total and reduced ascorbate found in *S. polyrhiza* treated plants could be one of the causes of these ameliorated conditions of membrane peroxidation in presence of MNPs, as the production and the regeneration of the pool of such non-enzymatic antioxidants is fundamental in determining the cellular redox state (Noctor and Foyer, 1998). In addition, the lower MDA concentration of MNP-exposed plants could imply a better functionality of the plasma-membrane itself, thus probably concurring to the previously mentioned increase in the acquisition of some nutrients. Nonetheless, these MNP-affected traits were only apparently positive, as *S. polyrhiza* treated plants showed a lower fresh and dry weight in respect to control plants as reported above.

4.2. MNP exposure triggers DNA methylation

PET particles at both concentrations induced a significant decrease in the number of U-loci, indicating that *S. polyrhiza* was undergoing DNA hypermethylation in presence of the studied contaminants. A similar response to MNPs have been found in animal in a recent study by Farag et al. (2023), while on plants the increase in methylations have been investigated and reported only in the case of other kinds of stress, such as heavy metals (Sun et al., 2021), salinity (Al-Lawati et al., 2016) and drought (Li R. et al., 2020). Interestingly, the PET-induced hypermethylation was mainly due to hemi-methylation (i.e. methylation of only one DNA strand) of the external cytosine of 5′-CCGG sites (i.e. one of the –CHG sites, where H = A, T or C; Muyle et al., 2022; Schulz et al., 2013), while no significant changes were reported between control and treated plants regarding hemi- or full methylation of the internal cytosine (i.e. –CG sites). A similar increase (about 50 %) in hemi-methylation was detected with MSAP technique in *S. polyrhiza* exposed to abscisic acid (ABA) for 5 days (Zhao et al., 2015). Considering that ABA is a broad-spectrum phytohormone that controls various stress responses (Agarwal and Jha, 2010) and induces the formation of turions in duckweeds (Wang and Messing, 2012), this result may suggest that the stressful PET-MNP exposure could prepare *S. polyrhiza* for dormancy possibly through a hormone-mediated pathway.

In addition, an increase in the methylation levels of –CHG contexts as a mechanism linked to the prevention of DNA damage has been proposed for *S. polyrhiza* when forming turions, as DNA-repairing enzymes are less active during dormancy (Pasaribu et al., 2023). Even if MSAP technique allowed us to study only one of the –CHG contexts (i.e. hemi-methylation of the external cytosine of 5′-CCGG sites), our results suggest that the general hypothesis of an increase in DNA methylation as a strategy to protect the genome from possible damages caused by dangerous products (i.e. ROS) (Sun et al., 2022) may be extended to the case of MNP stress. Since the cyto/genotoxicity of MNPs on higher plants has already been demonstrated (Giorgetti et al., 2020; Kaur et al., 2022; Maity et al., 2020) and linked to oxidative stress (Maity et al., 2023), DNA hypermethylation after PET-MNP exposure in *S. polyrhiza* could

have been triggered by the particle-imposed alteration of oxidative status, with the above mentioned aim of genome protection. Alternative hypothesis regarding the causes of this epigenetic modification should be developed following more comprehensive investigations in which the methylation-subjected genomic regions or genes could be identified (i.e. through MSAP-seq, Chwialkowska et al., 2017).

In any case, the molecular mechanisms responsible for de-novo methylation remain to be elucidated, considering that the canonical RNA-directed DNA methylation (RdDM) pathway has been lost by *S. polyrhiza* during evolution (Harkess et al., 2020). Considering the fast reproduction time of *S. polyrhiza*, the hemi-methylation here reported can be interpreted as full methylation on its way to completion. In fact, hemi-methylation is usually a result of DNA replication of a fully methylated DNA molecule (Kalisz and Purugganan, 2004) and full methylation is likely to be restored since the mechanism involved in its maintenance is normally present in the studied strain (i.e. 9509) (Harkess et al., 2020). This mechanism relies on a feedback loop between di-methylation of lysine 9 on histone 3 (H3K9me2) and the DNA methyltransferase CMT3 (Du et al., 2015; Harkess et al., 2020).

The here reported marked increase in the percentage of hemi-methylated external cytosines of 5′-CCGG sites in the presence of plastic particles could be implicated also in the creation of epialleles (i.e. alleles that differ in their degree of methylation (Kalisz and Purugganan, 2004). In fact, a variety of biotic and abiotic stresses can induce new epialleles (Srikant and Tri Wibowo, 2022), whose functions are not completely understood, since there is a complex relationship between changes in phenotype and changes in DNA methylation patterns (Medrano et al., 2014). In the case of *S. polyrhiza*, clonal reproduction allows an easy transmission of MNP-induced epigenetic modifications (e.g. hypermethylation) that might improve long-term resistance to these new generation pollutants. Recently, Van Antro et al. (2023) demonstrated that temperature stress-induced hypermethylation in -CHG contexts was maintained even after 3–12 generations in *Lemna minor* cultivated in controlled conditions. Transgenerational stress memory from exposure to MNPs could be thus expected and future long-term molecular studies are needed to confirm this hypothesis. Moreover, sequence-based identification of MNP-induced changes in DNA methylation are necessary to go further the MSAP screening of anonymous loci without specifying genomic regions or genes (Schrey et al., 2013).

5. Conclusions

The presence of PET-MNPs caused alterations in the growth and physiology of *Spirodela polyrhiza*, including reduction in fresh and dry weight, oxidative stress, photosynthesis impairment, changes in starch and element concentration. In addition, MNP-induced DNA hypermethylation was revealed through MSAP technique, indicating that this freshwater species was protecting its genome and/or creating new epialleles to counteract these xenobiotic stressing agents. This work represents the first demonstration that MNPs can have an impact on the epigenetic mechanisms in plant organisms. Long term studies are needed to understand the role of epigenetic modifications in MNP response and transgenerational stress memory.

CRediT authorship contribution statement

Marco Dainelli: Writing – review & editing, Writing – original draft, Methodology, Investigation, Formal analysis, Data curation, Conceptualization. **Maria Beatrice Castellani:** Writing – review & editing, Investigation, Formal analysis. **Sara Pignattelli:** Writing – review & editing, Formal analysis. **Sara Falsini:** Writing – review & editing, Investigation, Formal analysis. **Sandra Ristori:** Writing – review & editing, Investigation, Formal analysis. **Alessio Papini:** Writing – review & editing, Resources. **Ilaria Colzi:** Writing – review & editing, Resources, Funding acquisition, Data curation, Conceptualization. **Andrea Coppi:** Writing – review & editing, Resources, Project administration, Methodology, Data curation, Conceptualization. **Cristina Gonnelli:** Writing – review & editing, Writing – original draft, Supervision, Resources, Project administration, Methodology, Conceptualization.

Declaration of competing interest

The authors declare that they have no known competing financial interests or personal relationships that could have appeared to influence the work reported in this paper.

Data availability

Data will be made available on request.

Acknowledgements

This work was carried out within the RETURN Extended Partnership supported under the the Italian PNRR program, Mission 4 Component 2 Investment 1.3 funded from the European Union—NextGenerationEU (project RETURN PE3 – "Multi-risk science for resilient communities under a changing climate", project no. PE00000005). The publication was made with the contribution of the researcher Marco Dainelli with a research contract co-funded by the European Union PON Research and Innovation 2014–2020 in accordance with Article 24, paragraph 3a), of Law No. 240 of December 30, 2010, as amended, and Ministerial Decree No. 1062 of August 10, 2021.

The authors are grateful to Klaus-J Appenroth for his useful advice on *S. polyrhiza* culturing.

Appendix A. Supplementary data

Supplementary data to this article can be found online at https://doi.org/10.1016/j.plaphy.2024.108403.

References

Agarwal, P.K., Jha, B., 2010. Transcription factors in plants and ABA dependent and independent abiotic stress signalling. Biol. Plant. (Prague) 54, 201–212. https://doi.org/10.1007/s10535-010-0038-7.

Alexieva, V., Sergiev, I., Mapelli, S., Karanov, E., 2001. The effect of drought and ultraviolet radiation on growth and stress markers in pea and wheat. Plant Cell Environ. 24, 1337–1344. https://doi.org/10.1046/j.1365-3040.2001.00778.x.

Al-Lawati, A., Al-Bahry, S., Victor, R., Al-Lawati, A.H., Yaish, M.W., 2016. Salt Stress Alters DNA Methylation Levels in Alfalfa (*Medicago* Spp). https://doi.org/10.4238/gmr.15018299.

Alonso, C., Pérez, R., Bazaga, P., Medrano, M., Herrera, C.M., 2016. MSAP markers and global cytosine methylation in plants: a literature survey and comparative analysis for a wild-growing species. Molecular Ecology Resources 16 (1), 80–90. https://doi.org/10.1111/1755-0998.12426.

An, D., Zhou, Y., Li, C., Xiao, Q., Wang, T., Zhang, Y., Wu, Y., Li, Y., Chao, D., Messing, J., Wang, W., 2019. Plant evolution and environmental adaptation unveiled by long-read whole-genome sequencing of *Spirodela*. Proc. Natl. Acad. Sci. USA 116 (38), 18893–18899. https://doi.org/10.1073/pnas.1910401116.

Anbumani, S., Kakkar, P., 2018. Ecotoxicological effects of microplastics on biota: a review. Environ. Sci. Pollut. Control Ser. 25, 14373–14396. https://doi.org/10.1007/s11356-018-1999-x.

Appenroth, K.J., Teller, S., Horn, M., 1996. Photophysiology of turion formation and germination in *Spirodela polyrhiza*. Biol. Plantarum 38, 95–106. https://doi.org/10.1007/BF02879642.

Appenroth, K.J., Krech, K., Keresztes, A., Fischer, W., Koloczek, H., 2010. Effects of nickel on the chloroplasts of the duckweeds *Spirodela polyrhiza* and *Lemna minor* and their possible use in biomonitoring and phytoremediation. Chemosphere 78 (3), 216–223. https://doi.org/10.1016/j.chemosphere.2009.11.007.

Appenroth, K.J., Keresztes, A., Krzysztofowicz, E., Gabrys, H., 2011. Light-induced degradation of starch granules in turions of *Spirodela polyrhiza* studied by electron microscopy. Plant Cell Physiol. 52 (2), 384–391. https://doi.org/10.1093/pcp/pcq199.

Arikan, B., Alp, F.N., Ozfidan-Konakci, C., Yildiztugay, E., Turan, M., Cavusoglu, H., 2022. The impacts of nanoplastic toxicity on the accumulation, hormonal regulation and tolerance mechanisms in a potential hyperaccumulator - *Lemna minor* L. J. Hazard Mater. 440, 129692 https://doi.org/10.1016/j.jhazmat.2022.129692.

Besseling, E., Quik, J.T.K., Sun, M., Koelmans, A.A., 2017. Fate of nano- and microplastic in freshwater systems: a modeling study. Environ. Pollut. 220, 540–548. https://doi.org/10.1016/j.envpol.2016.10.001.

Bettarini, I., Colzi, I., Coppi, A., Falsini, S., Echevarria, G., Pazzagli, L., Selvi, F., Gonnelli, C., 2019. Unravelling soil and plant metal relationships in Albanian nickel hyperaccumulators in the genus *Odontarrhena* (syn. *Alyssum* sect. *Odontarrhena*, Brassicaceae). Plant Soil 440, 135–149. https://doi.org/10.1007/s11104-019-04077-y.

Bornette, G., Puijalon, S., 2009. Macrophytes: ecology of aquatic plants. In: ELS. Wiley. https://doi.org/10.1002/9780470015902.a0020475.

Bussotti, F., Hazeem Kalaji, M., Desotgiu, R., Pollastrini, M., Loboda, T., Bosa, K., 2012. Fattori ambientali e parametri di fluorescenza. In: Misurare la Vitalità delle Piante per Mezzo della Fluorescenza della Clorofilla, vol. 2012. Firenze University Press, Firenze, Italy. https://doi.org/10.36253/978-88-6655-216-1.

Cao, X.H., Vu, G.T.H., 2020. Cytogenetics, epigenetics and karyotype evolution of duckweeds. In: Cao, X., Fourounjian, P., Wang, W. (Eds.), The Duckweed Genomes. Compendium of Plant Genomes. Springer, Cham. https://doi.org/10.1007/978-3-030-11045-1_4.

Chwialkowska, K., Korotko, U., Kosinska, J., Szarejko, I., Kwasniewski, M., 2017. Methylation sensitive amplification polymorphism sequencing (MSAP-Seq)—a method for high-throughput analysis of differentially methylated CCGG sites in plants with large genomes. Front. Plant Sci. 8, 2056. https://doi.org/10.3389/fpls.2017.02056.

Colzi, I., Renna, L., Bianchi, E., Castellani, M.B., Coppi, A., Pignattelli, S., Loppi, S., Gonnelli, C., 2022. Impact of microplastics on growth, photosynthesis and essential elements in *Cucurbita pepo* L. J. Hazard Mater. 423, 127238 https://doi.org/10.1016/j.jhazmat.2021.127238.

Colpo, A., Demaria, S., Baldisserotto, C., Pancaldi, S., Brestič, M., Živčak, M., Ferroni, L., 2023. Long-term alleviation of the functional phenotype in chlorophyll-deficient wheat and impact on productivity: a semi-field phenotyping experiment. Plants 12, 822. https://doi.org/10.3390/plants12040822.

Cui, R., Kwak, J.I., An, Y.-J., 2023. Multigenerational effects of microplastic fragments derived from polyethylene terephthalate bottles on duckweed *Lemna minor*: size-dependent effects of microplastics on photosynthesis. Sci. Total Environ. 872, 162159 https://doi.org/10.1016/j.scitotenv.2023.162159.

Cui, Q., Wang, F., Wang, X., Chen, T., Guo, X., 2023. Environmental toxicity and ecological effects of micro(nano)plastics: a huge challenge posed by biodegradability. TrAC, Trends Anal. Chem. 164, 117092 https://doi.org/10.1016/j.trac.2023.117092.

Dainelli, M., Pignattelli, S., Bazihizina, N., Falsini, S., Papini, A., Baccelli, I., Mancuso, S., Coppi, A., Castellani, M.B., Colzi, I., Gonnelli, C., 2023. Can microplastics threaten plant productivity and fruit quality? Insights from Micro-Tom and Micro-PET/PVC. Sci. Total Environ. 895, 165118 https://doi.org/10.1016/j.scitotenv.2023.165119.

Dey, S., Guha, T., Barman, F., Natarajan, L., Kundu, R., Mukherjee, A., Paul, S., 2023. Surface functionalization and size of polystyrene microplastics concomitantly regulate growth, photosynthesis and anti-oxidant status of *Cicer arietinum* L. Plant Physiol. Biochem. 194, 41–51. https://doi.org/10.1016/j.plaphy.2022.11.004.

Dovidat, L.C., Brinkmann, B.W., Vijver, M.G., Bosker, T., 2020. Plastic particles adsorb to the roots of freshwater vascular plant *Spirodela polyrhiza* but do not impair growth. Limnol Oceanogr Lett 5, 37–45. https://doi.org/10.1002/lol2.10118.

Du, J., Johnson, L.M., Jacobsen, S.E., Patel, D.J., 2015. DNA methylation pathways and their crosstalk with histone methylation. Nat. Rev. Mol. Cell Biol. 16, 519–532. https://doi.org/10.1038/nrm4043.

Egbeocha, C., Malek, S., Emenike, C., Milow, P., 2018. Feasting on microplastics: ingestion by and effects on marine organisms. Aquat. Biol. 27, 93–106. https://doi.org/10.3354/ab00701.

Ekvall, M.T., Lundqvist, M., Kelpsiene, E., Šileikis, E., Gunnarsson, S.B., Cedervall, T., 2019. Nanoplastics formed during the mechanical breakdown of daily-use polystyrene products. Nanoscale Adv. 1 (3), 1055–1061. https://doi.org/10.1039/C8NA00210J.

Excoffier, L., Lischer, H.E., 2010. Arlequin suite ver 3.5: a new series of programs to perform population genetics analyses under Linux and Windows. Mol Ecol Resour 10 (3), 564–567. https://doi.org/10.1111/j.1755-0998.2010.02847.x.

Falsini, S., Colzi, I., Chelazzi, D., Dainelli, M., Schiff, S., Papini, A., Coppi, A., Gonnelli, C., Ristori, S., 2022. Plastic is in the air: impact of micro-nanoplastics from airborne pollution on *Tillandsia usneoides* (L.) L. (Bromeliaceae) as a possible green sensor. J. Hazard Mater. 437, 129314 https://doi.org/10.1016/j.jhazmat.2022.129314.

Farag, A.A., Youssef, H.S., Sliem, R.E., El Gazzar, W.B., Nabil, N., Mokhtar, M.M., Marei, Y.M., Ismail, N.S., Radwaan, S.E., Badr, A.M., Sayed, A.E.-D.H., 2023. Hematological consequences of polyethylene microplastics toxicity in male rats: oxidative stress, genetic, and epigenetic links. Toxicology 492, 153545. https://doi.org/10.1016/j.tox.2023.153545.

Fu, Q., Lai, J.L., Ji, X.H., Luo, Z.X., Wu, G., Luo, X.G., 2022. Alterations of the rhizosphere soil microbial community composition and metabolite profiles of *Zea mays* by polyethylene-particles of different molecular weights. J. Hazard Mater. 423, 127062 https://doi.org/10.1016/j.jhazmat.2021.127062.

Giorgetti, L., Spanò, C., Muccifora, S., Bottega, S., Barbieri, F., Bellani, L., Castiglione, M. F., 2020. Exploring the interaction between polystyrene nanoplastics and *Allium cepa* during germination: internalization in root cells, induction of toxicity and oxidative stress. Plant Physiol. Biochem. 148, 170–177. https://doi.org/10.1016/j.plaphy.2020.02.014.

Gomes, A.R., Freitas, Í.N., Luz, T.M. da, Guimarães, A.T.B., Araújo, A.P. da C., Kamaraj, C., Rahman, MdM., Islam, A.R.MdT., Arias, A.H., Silva, F.B. da, Karthi, S., Cruz-Santiago, O., Silva, F.G., Malafaia, G., 2023. Multiple endpoints of polyethylene microplastics toxicity in vascular plants of freshwater ecosystems: a study involving *Salvinia auriculata* (Salviniaceae). J. Hazard Mater. 450, 131069 https://doi.org/10.1016/j.jhazmat.2023.131069.

Gupta, D.K., Choudhary, D., Vishwakarma, A., Mudgal, M., Srivastava, A.K., Singh, A., 2022. Microplastics in freshwater environment: occurrence, analysis, impact, control measures and challenges. Int. J. Environ. Sci. Technol. 20, 6865–6896. https://doi.org/10.1007/s13762-022-04139-2.

Harkess, A., Bewick, A.J., Lu, Z., Fourounjian, P., Messing, J., Michael, T.P., Schmitz, R. J., Meyers, B.C., 2020. Unusual predominance of maintenance DNA methylation in *Spirodela polyrhiza*. bioRxiv. https://doi.org/10.1101/2020.12.03.410332.

Heath, R.L., Packer, L., 1968. Photoperoxidation in isolated chloroplasts. Arch. Biochem. Biophys. 125, 189–198. https://doi.org/10.1016/0003-9861(68)90654-1.

Iannilli, V., Passatore, L., Carloni, S., Lecce, F., Sciacca, G., Zacchini, M., Pietrini, F., 2023. Microplastic toxicity and trophic transfer in freshwater organisms: ecotoxicological and genotoxic assessment in *Spirodela polyrhiza* (L.) Schleid. And *Echinogammarus veneris* (Heller, 1865) treated with polyethylene microparticles. Water (Basel) 15, 921. https://doi.org/10.3390/w15050921.

Ilechukwu, I., Ehigiator, B.E., Ben, I.O., Okonkwo, C.J., Olorunfemi, O.S., Modo, U.E., Ilechukwu, C.E., Ohagwa, N.J., 2022. Chronic toxic effects of polystyrene microplastics on reproductive parameters of male rats. Environ Anal Health Toxicol 37, e2022015. https://doi.org/10.5620/eaht.2022015.

Im, J., Eom, H.-J., Choi, J., 2022. Effect of early-life exposure of polystyrene microplastics on behavior and DNA methylation in later life stage of zebrafish. Arch. Environ. Contam. Toxicol. 82, 558–568. https://doi.org/10.1007/s00244-022-00924-9.

Kalčíková, G., 2020a. Aquatic vascular plants – a forgotten piece of nature in microplastic research. Environ. Pollut. 262, 114354 https://doi.org/10.1016/j.envpol.2020.114354.

Kalčíková, G., Skalar, T., Marolt, G., Jemec Kokalj, A., 2020b. An environmental concentration of aged microplastics with adsorbed silver significantly affects aquatic organisms. Water Res. 175, 115644 https://doi.org/10.1016/j.watres.2020.115644.

Kalisz, S., Purugganan, M.D., 2004. Epialleles via DNA methylation: consequences for plant evolution. Trends Ecol. Evol. 19 (6), 309–314. https://doi.org/10.1016/j.tree.2004.03.034.

Kaur, M., Xu, M., Wang, L., 2022. Cyto–genotoxic effect causing potential of polystyrene micro-plastics in terrestrial plants. Nanomaterials 12, 2024. https://doi.org/10.3390/nano12122024.

Kiran, B.R., Kopperi, H., Venkata Mohan, S., 2022. Micro/nano-plastics occurrence, identification, risk analysis and mitigation: challenges and perspectives. Rev. Environ. Sci. Biotechnol. 21, 169–203. https://doi.org/10.1007/s11157-021-09609-6.

Law, M.Y., Charles, S.A., Halliwell, B., 1983. Glutathione and ascorbic acid in spinach (*Spinacia oleracea)* chloroplasts. The effect of hydrogen peroxide and of Paraquat. Biochem. J. 210, 899–903. https://doi.org/10.1042/bj2100899.

Li, C., Busquets, R., Campos, L.C., 2020. Assessment of microplastics in freshwater systems: a review. Sci. Total Environ. 707, 135578 https://doi.org/10.1016/j.scitotenv.2019.135578.

Li, R., Hu, F., Li, B., Zhang, Y., Chen, M., Fan, T., Wang, T., 2020. Whole genome bisulfite sequencing methylome analysis of mulberry (*Morus alba*) reveals epigenome modifications in response to drought stress. Sci. Rep. 10, 8013. https://doi.org/10.1038/s41598-020-64975-5.

Lian, J., Liu, W., Sun, Y., Men, S., Wu, J., Zeb, A., Yang, T., Ma, L.Q., Zhou, Q., 2022. Nanotoxicological effects and transcriptome mechanisms of wheat (*Triticum aestivum* L.) under stress of polystyrene nanoplastics. J. Hazard Mater. 423 (B), 127241 https://doi.org/10.1016/j.jhazmat.2021.127241.

Liu, Y., Sanguanphun, T., Yuan, W., Cheng, J.J., Meetam, M., 2017. The biological responses and metal phytoaccumulation of duckweed *Spirodela polyrhiza* to manganese and chromium. Environ. Sci. Pollut. Control Ser. 24, 19104–19113. https://doi.org/10.1007/s11356-017-9519-y.

López de las Hazas, M.-C., Boughanem, H., Dávalos, A., 2022. Untoward effects of micro- and nanoplastics: an expert review of their biological impact and epigenetic effects. Adv. Nutr. 13, 1310–1323. https://doi.org/10.1093/advances/nmab154.

Maity, S., Guchhait, R., De, S., Pramanick, K., 2023. High doses of nano-polystyrene aggravate the oxidative stress, DNA damage, and the cell death in onions. Environ. Pollut. 316 (2), 120611 https://doi.org/10.1016/j.envpol.2022.120611.

Maity, S., Chatterjee, A., Guchhait, R., De, S., Pramanick, K., 2020. Cytogenotoxic potential of a hazardous material, polystyrene microparticles on *Allium cepa* L. J. Hazard Mater. 385, 121560 https://doi.org/10.1016/j.jhazmat.2019.121560.

Martín, C., Pirredda, M., Fajardo, C., Costa, G., Sánchez-Fortún, S., Nande, M., Mengs, G., Martín, M., 2023. Transcriptomic and physiological effects of polyethylene microplastics on *Zea mays* seedlings and their role as a vector for organic pollutants. Chemosphere 322, 138167. https://doi.org/10.1016/j.chemosphere.2023.138167.

Mateos-Cárdenas, A., Scott, D.T., Seitmaganbetova, G., Frank, N.A.M., van, P., John, O., Marcel, A.K.J., 2019. Polyethylene microplastics adhere to *Lemna minor* (L.), yet have no effects on plant growth or feeding by *Gammarus duebeni* (Lillj.). Sci. Total Environ. 689, 413–421. https://doi.org/10.1016/j.scitotenv.2019.06.359.

Medrano, M., Herrera, C.M., Bazaga, P., 2014. Epigenetic variation predicts regional and local intraspecific functional diversity in a perennial herb. Mol. Ecol. 23 (20), 4926–4938. https://doi.org/10.1111/mec.12911.

Michael, T.P., Bryant, D., Gutierrez, R., Borisjuk, N., Chu, P., Zhang, H., Xia, J., Zhou, J., Peng, H., El Baidouri, M., Ten Hallers, B., Hastie, A.R., Liang, T., Acosta, K., Gilbert, S., McEntee, C., Jackson, S.A., Mockler, T.C., Zhang, W., Lam, E., 2017. Comprehensive definition of genome features in *Spirodela polyrhiza* by high-depth physical mapping and short-read DNA sequencing strategies. Plant J.: for cell and molecular biology 89 (3), 617–635. https://doi.org/10.1111/tpj.13400.

Miller, M.E., Hamann, M., Kroon, F.J., 2020. Bioaccumulation and biomagnification of microplastics in marine organisms: a review and meta-analysis of current data. PLoS One 15, e0240792. https://doi.org/10.1371/journal.pone.0240792.

My Tran, N., Thanh Hoai Ta, Q., Sreedhar, A., Noh, J.-S., 2021. Ti3C2Tx MXene playing as a strong methylene blue adsorbent in wastewater. Appl. Surf. Sci. 537, 148006 https://doi.org/10.1016/j.apsusc.2020.148006.

Monteiro, S.S., Pinto da Costa, J., 2022. Methods for the extraction of microplastics in complex solid, water and biota samples. Trends in Environmental Analytical Chemistry 33, e00151. https://doi.org/10.1016/j.teac.2021.e00151.

Muyle, A.M., Seymour, D.K., Lv, Y., Huettel, B., Gaut, B.S., 2022. Gene body methylation in plants: mechanisms, functions, and important implications for understanding evolutionary processes. Genome Biology and Evolution 14 (4), evac038. https://doi.org/10.1093/gbe/evac038.

Noctor, G., Foyer, C.H., 1998. Ascorbate and glutathione: keeping active oxygen under control. Annu. Rev. Plant Physiol. Plant Mol. Biol. 49, 249–279. https://doi.org/10.1146/annurev.arplant.49.1.249.

OECD, 2022. Global Plastics Outlook. OECD. https://doi.org/10.1787/de747aef-en.

OECD, 2006. Test No. 221: *Lemna* Sp. Growth Inhibition Test. OECD. https://doi.org/10.1787/9789264016194-en.

Oláh, V., Irfan, M., Szabó, Z.B., Sajtos, Z., Ragyák, Á.Z., Döncző, B., Jansen, M.A.K., Szabó, S., Mészáros, I., 2023. Species- and metal-specific responses of the ionome of three duckweed species under chromate and nickel treatments. Plants 12 (180). https://doi.org/10.3390/plants12010180.

Pasaribu, B., Acosta, K., Aylward, A., Liang, Y., Abramson, B.W., Colt, K., Hartwick, N.T., Shanklin, J., Michael, T.P., Lam, E., 2023. Genomics of turions from the Greater Duckweed reveal its pathways for dormancy and re-emergence strategy. New Phytol. 239 (1), 116–131. https://doi.org/10.1111/nph.18941.

Patrício Silva, A.L., Prata, J.C., Walker, T.R., Duarte, A.C., Ouyang, W., Barcelò, D., Rocha-Santos, T., 2021. Increased plastic pollution due to COVID-19 pandemic: challenges and recommendations. Chem. Eng. J. 405, 126683 https://doi.org/10.1016/j.cej.2020.126683.

Rana, Q.u. a., Khan, M.A.N., Irfan, M., Shah, A.A., Hasan, F., Khan, S., Ahmed, S., Adnan, F., Li, W., Ju, M., Badshah, M., 2021. Starved *Spirodela polyrhiza* and *Saccharomyces cerevisiae*: a potent combination for sustainable bioethanol production. Biomass Conv. Bioref. 11, 1665–1674. https://doi.org/10.1007/s13399-019-00540-z.

Raza, A., Ashraf, F., Zou, X., Zhang, X., Tosif, H., 2020. Plant adaptation and tolerance to environmental stresses: mechanisms and perspectives. In: Plant Ecophysiology and Adaptation under Climate Change: Mechanisms and Perspectives I. Springer Singapore, Singapore, pp. 117–145. https://doi.org/10.1007/978-981-15-2156-0_5.

Rivas, M.L., Albion, I., Bernal, B., Handcock, R.N., Heatwole, S.J., Parrott, M.L., Piazza, K.A., Deschaseaux, E., 2022. The plastic pandemic: COVID-19 has accelerated plastic pollution, but there is a cure. Sci. Total Environ. 847, 157555 https://doi.org/10.1016/j.scitotenv.2022.157555.

Rozman, U., Jemec Kokalj, A., Dolar, A., Drobne, D., Kalčíková, G., 2022. Long-term interactions between microplastics and floating macrophyte *Lemna minor*: the potential for phytoremediation of microplastics in the aquatic environment. Sci. Total Environ. 831, 154866 https://doi.org/10.1016/j.scitotenv.2022.154866.

Schindelin, J., Arganda-Carreras, I., Frise, E., Kaynig, V., Longair, M., Pietzsch, T., Preibisch, S., Rueden, C., Saalfeld, S., Schmid, B., Tinevez, J.-Y., White, D.J., Hartenstein, V., Eliceiri, K., Tomancak, P., Cardona, A., 2012. Fiji: an open-source platform for biological-image analysis. Nat. Methods 9, 676–682. https://doi.org/10.1038/nmeth.2019.

Schreinemakers, W.A.C., 1984. Effects of metal ions on growth of and on ion absorption by *Spirodela polyrhiza* (L.) schleiden effects of iron, magnesium and zinc. Z. Pflanzenphysiol. 114 (2), 123–129. https://doi.org/10.1016/S0044-328X(84)80025-2.

Schrey, A.W., Alvarez, M., Foust, C.M., Kilvitis, H.J., Lee, J.D., Liebl, A.L., Martin, L.B., Richards, C.L., Robertson, M., 2013. Ecological epigenetics: beyond MS-AFLP. Integr. Comp. Biol. 53, 340–350. https://doi.org/10.1093/icb/ict012.

Schulz, B., Eckstein, R.L., Durka, W., 2013. Scoring and analysis of methylation-sensitive amplification polymorphisms for epigenetic population studies. Molecular Ecology Resources 13 (4), 642–653. https://doi.org/10.1111/1755-0998.12100.

Sedlak, J., Lindsay, R.H., 1968. Estimation of total, protein-bound, and nonprotein sulfhydryl groups in tissue with Ellman's reagent. Anal. Biochem. 25, 192–205. https://doi.org/10.1016/0003-2697(68)90092-4.

Senavirathna, M.D.H.J., Zhaozhi, L., Fujino, T., 2022. Root adsorption of microplastic particles affects the submerged freshwater macrophyte *Egeria densa*. Water Air Soil Pollut. 233, 80. https://doi.org/10.1007/s11270-022-05556-2.

Sitko, R., Turek, E., Zawisza, B., Malicka, E., Talik, E., Heimann, J., Gagor, A., Feist, B., Wrzalik, R., 2013. Adsorption of divalent metal ions from aqueous solutions using graphene oxide. Dalton Trans. 42, 5682. https://doi.org/10.1039/c3dt33097d.

Song, Y.K., Hong, S.H., Eo, S., Han, G.M., Shim, W.J., 2020. Rapid production of micro- and nanoplastics by fragmentation of expanded polystyrene exposed to sunlight. Environ. Sci. Technol. 54 (18), 11191–11200. https://doi.org/10.1021/acs.est.0c02288.

Srikant, T., Tri Wibowo, A., 2022. The underlying nature of epigenetic variation: origin, establishment, and regulatory function of plant epialleles. Int. J. Mol. Sci. 22, 8618. https://doi.org/10.3390/ijms22168618.

Stirbet, A., Govindjee, 2011. On the relation between the Kautsky effect (chlorophyll a fluorescence induction) and Photosystem II: basics and applications of the OJIP fluorescence transient. J. Photochem. Photobiol. B Biol. 104 (1–2), 236–257. https://doi.org/10.1016/j.jphotobiol.2010.12.010.

Strasser, R.J., Srivastava, A., Tsimilli-Michael, M., 2000. The fluorescence transient as a tool to characterize and screen photosynthetic samples. In: Probing Photosynthesis: Mechanism, Regulation & Adaptation, vol. 2000. Taylor and Francis, London UK. New York, NY, USA, pp. 445–483.

Squadrone, S., Pederiva, S., Bezzo, T., Mussat Sartor, R., Battuello, M., Nurra, N., Griglione, A., Brizio, P., Abete, M.C., 2021. Microplastics as vectors of metals contamination in Mediterranean Sea. Environ. Sci. Pollut. Res. https://doi.org/10.1007/s11356-021-13662-7.

Sun, M., Yang, Z., Liu, L., Duan, L., 2022. DNA methylation in plant responses and adaption to abiotic stresses. Int. J. Mol. Sci. 23, 6910. https://doi.org/10.3390/ijms23136910.

Sun, D., Sun, J., Huang, L., Chen, N., Wang, Q., 2021. Effects of cadmium stress on DNA methylation in soybean. Biotechnol. Biotechnol. Equip. 35 (1), 1696–1705. https://doi.org/10.1080/13102818.2021.1980107.

Tang, M., Huang, Y., Zhang, W., Fu, T., Zeng, T., Huang, Y., Yang, X., 2022. Effects of microplastics on the mineral elements absorption and accumulation in hydroponic rice seedlings (*Oryza sativa* L.). Bull. Environ. Contam. Toxicol. 108, 949–955. https://doi.org/10.1007/s00128-021-03453-8.

Thiebaut, F., Hemerly, A.S., Ferreira, P.C.G., 2019. A role for epigenetic regulation in the adaptation and stress responses of non-model plants. Front. Plant Sci. 10, 246. https://doi.org/10.3389/fpls.2019.00246.

Teng, L., Zhu, Y., Li, H., Song, X., Shi, L., 2022. The phytotoxicity of microplastics to the photosynthetic performance and transcriptome profiling of *Nicotiana tabacum* seedlings. Ecotoxicol. Environ. Saf. 231, 113155 https://doi.org/10.1016/j.ecoenv.2021.113155.

Van Antro, M., Prelovsek, S., Ivanovic, S., Gawehns, F., Wagemaker, N.C.A.M., Mysara, M., Horemans, N., Vergeer, P., Verhoeven, K.J.F., 2023. DNA methylation in clonal duckweed (*Lemna minor* L.) lineages reflects current and historical environmental exposures. Mol. Ecol. 32 (2), 428–443. https://doi.org/10.1111/mec.16757.

van Weert, S., Redondo-Hasselerharm, P.E., Diepens, N.J., Koelmans, A.A., 2019. Effects of nanoplastics and microplastics on the growth of sediment-rooted macrophytes. Sci. Total Environ. 654, 1040–1047. https://doi.org/10.1016/j.scitotenv.2018.11.183.

Vanyushin, B.F., Ashapkin, V.V., 2011. DNA methylation in higher plants: past, present and future. Biochimica et Biophysica Acta (BBA) - Gene Regulatory Mechanisms 1809, 360–368. https://doi.org/10.1016/j.bbagrm.2011.04.006.

Vos, P., Hogers, R., Bleeker, M., Reijans, M., van de Lee, T., Hornes, M., Frijters, A., Pot, J., Peleman, J., Kuiper, M., Zabeau, M., 1995. AFLP: a new technique for DNA fingerprinting. Nucleic Acids Res. 23 (21), 4407–4414. https://doi.org/10.1093/nar/23.21.4407.

Wang, J., Lu, S., Bian, H., Xu, M., Zhu, W., Wang, H., He, C., Sheng, L., 2022. Effects of individual and combined polystyrene nanoplastics and phenanthrene on the enzymology, physiology, and transcriptome parameters of rice (*Oryza sativa* L.). Chemosphere 304, 135341. https://doi.org/10.1016/j.chemosphere.2022.135341.

Wang, L., Gao, Y., Jiang, W., Chen, J., Chen, Y., Zhang, X., Wang, G., 2021. Microplastics with cadmium inhibit the growth of *Vallisneria natans* (Lour.) Hara rather than reduce cadmium toxicity. Chemosphere 266, 128979. https://doi.org/10.1016/j.chemosphere.2020.128979.

Wang, Q., Zhang, C., Li, R., 2023. Plastic pollution induced by the COVID-19: environmental challenges and outlook. Environ. Sci. Pollut. Control Ser. 30, 40405–40426. https://doi.org/10.1007/s11356-022-24901-w.

Wang, W., Messing, J., 2012. Analysis of ADP-glucose pyrophosphorylase expression during turion formation induced by abscisic acid in *Spirodela polyrhiza* (greater duckweed). BMC Plant Biol. 12, 5. https://doi.org/10.1186/1471-2229-12-5.

Wang, Y., Bai, J., Wen, L., Wang, W., Zhang, L., Liu, Z., Liu, H., 2023a. Phytotoxicity of microplastics to the floating plant *Spirodela polyrhiza* (L.): plant functional traits and metabolomics. Environ. Pollut. 322, 121199 https://doi.org/10.1016/j.envpol.2023.121199.

Wang, Y., Xiang, L., Wang, F., Redmile-Gordon, M., Bian, Y., Wang, Z., Gu, C., Jiang, X., Schäffer, A., Xing, B., 2023b. Transcriptomic and metabolomic changes in lettuce triggered by microplastics-stress. Environ. Pollut. 320, 121081 https://doi.org/10.1016/j.envpol.2023.121081.

Wang, Y., Xiang, L., Wang, F., Wang, Z., Bian, Y., Gu, C., Wen, X., Kengara, F.O., Schäffer, A., Jiang, X., Xing, B., 2022. Positively charged microplastics induce strong lettuce stress responses from physiological, transcriptomic, and metabolomic perspectives. Environ. Sci. Technol. 56, 16907–16918. https://doi.org/10.1021/acs.est.2c06054.

Wu, W.-M., Yang, J., Criddle, C.S., 2017. Microplastics pollution and reduction strategies. Front. Environ. Sci. Eng. 11, 6. https://doi.org/10.1007/s11783-017-0897-7.

Xiao, F., Feng, L.-J., Sun, X.-D., Wang, Y., Wang, Z.-W., Zhu, F.-P., Yuan, X.-Z., 2022. Do polystyrene nanoplastics have similar effects on duckweed (*Lemna minor* L.) at environmentally relevant and observed-effect concentrations? Environ. Sci. Technol. 56, 4071–4079. https://doi.org/10.1021/acs.est.1c06595.

Xu, Y.-L., Fang, Y., Li, Q., Yang, G.-L., Guo, L., Chen, G.-K., Tan, L., Jin, Y.-I., Zhao, H., 2018. Turion, an innovative duckweed-based starch production system for economical biofuel manufacture. Ind. Crop. Prod. 124, 108–114. https://doi.org/10.1016/j.indcrop.2018.07.061.

Yin, L., Wen, X., Huang, D., Du, C., Deng, R., Zhou, Z., Tao, J., Li, R., Zhou, W., Wang, Z., Chen, H., 2021. Interactions between microplastics/nanoplastics and vascular plants. Environ. Pollut. 290, 117999 https://doi.org/10.1016/j.envpol.2021.117999.

Yu, H., Qi, W., Cao, X., Wang, Y., Li, Y., Xu, Y., Zhang, X., Peng, J., Qu, J., 2022. Impact of microplastics on the foraging, photosynthesis and digestive systems of submerged carnivorous macrophytes under low and high nutrient concentrations. Environ. Pollut. 292, 118220 https://doi.org/10.1016/j.envpol.2021.118220.

Zhang, L., Li, Y., Wang, W., Zhang, W., Zuo, Q., Abdelkader, A., Xi, K., Heynderickx, P. M., Kim, K., 2021. The potential of microplastics as adsorbents of sodium dodecyl benzene sulfonate and chromium in an aqueous environment. Environ. Res. 197, 111057 https://doi.org/10.1016/j.envres.2021.111057.

Zhang, H., Lang, Z., Zhu, J.-K., 2018. Dynamics and function of DNA methylation in plants. Nat. Rev. Mol. Cell Biol. 19, 489–506. https://doi.org/10.1038/s41580-018-0016-z.

Zhao, Z., Shi, H.J., Wang, M.L., Cui, L., Yang, Z.G., Zhao, Y., 2015. Analysis of DNA methylation of *Spirodela polyrhiza* (Grater Duckweed) in response to abscisic acid using methylation-sensitive amplied polymorphism. Russ. J. Plant Physiol. 62, 127–135. https://doi.org/10.1134/S1021443715010197.

Zhou, J., Liu, X., Jiang, H., Li, X., Li, W., Cao, Y., 2022. Antidote or Trojan horse for submerged macrophytes: role of microplastics in copper toxicity in aquatic environments. Water Res. 216, 118354 https://doi.org/10.1016/j.watres.2022.118354.